Heliyon 10 (2024) e39532

Contents lists available at ScienceDirect

Heliyon

journal homepage: www.cell.com/heliyon

Research article

RNAs m^{6}A modification facilitates UVB-induced photoaging

Shuping Zhang [a], Meng Wu [b,c], Tingting Lu [a], Xiaoying Tian [a], Lihua Gao [a], Siyu Yan [a], Dan Wang [a], Jinrong Zeng [a,**], Lina Tan [a,*]

[a] Department of Dermatology, Postdoctoral Station of Clinical Medicine, The Third Xiangya Hospital of Central South University, Changsha, 410013, Hunan, China
[b] Department of Dermatology, Xiangya Hospital of Central South University, Changsha, 410008, Hunan, China
[c] Department of Dermatology, Hunan Provincial People's Hospital of Hunan Normal University, Changsha, 410005, Hunan, China

ARTICLE INFO

Keywords:
N6-methylation
Methyltransferases
METTL3
METTL14
Photoaging

ABSTRACT

RNA N6-methylation (m^{6}A) modification is common in eukaryotic mRNA and has been linked to various physiological disorders, including UVB-induced photoaging. To identify biological differences among photoaging. Three pairs of normal and photoaged skin tissues were collected for m^{6}A RNA sequencing assay. Transcriptome profiles showed differential m^{6}A methylation modifications in 1365 mRNAs in photoaging skin tissues. Pathway analysis revealed the involvement of cellular stress response and regulation of cell cycle G2/M phase transition in m^{6}A-mRNAs. Further experiments validated the differential expression of m^{6}A methyltransferases (METTL3 and METTL14) and hypermethylation modification in mRNAs (CENPE, PPM1B and TPM1). *In vitro* studies demonstrated that increased METTL3 and METTL14 levels promoted m^{6}A methylation of CENPE, PPM1B and TPM1 in UVB-induced photoaging cells, and further experiments on mice showed that downregulation of METTL3 and METTL14 reduced m^{6}A modifications in CENPE, PPM1B and TPM1, leading to the delayed appearance of photoaging phenotypes, suggesting that these genes could serve as potential therapeutic targets for treating photoaging. Our study characterized key transcriptome changes in photoaging and identified the role of METTL3 and METTL14 in mediating m^{6}A modification, resulting in the upregulation of CENPE, PPM1B and TPM1 expression, which may be crucial in UVB-induced photoaging.

1. Introduction

Skin aging can be classified into two main categories: endogenous aging, which occurs naturally with age, and exogenous aging, which is primarily caused by external factors such as exposure to ultraviolet (UV) radiation. The cumulative of UV light on the skin leading to various detrimental effects, including the production of reactive oxygen species (ROS) [1,2], DNA damage and collagen degradation [3,4], which can lead to various conditions such as melasma, solar keratosis and even skin tumors [5,6]. Despite the evident impact of UV-induced photoaging, the underlying mechanisms are not yet fully understood. Thus, further research on post-transcriptional gene regulation can deepen our understanding of the molecular basis of skin photoaging, which may facilitate the development of comprehensive anti-aging strategies and interventions aimed at delaying age-related skin phenotypes.

The loss of structural integrity and changes in phenotypic and physiological traits in the skin are influenced by both intrinsic and

* Corresponding author.
** Corresponding author.
E-mail address: tanlinawork@163.com (L. Tan).

https://doi.org/10.1016/j.heliyon.2024.e39532
Received 1 June 2024; Received in revised form 8 October 2024; Accepted 16 October 2024
Available online 18 October 2024

extrinsic factors [7]. Among extrinsic factors, UVB radiation primarily affects the epidermis and gradually induces photoaging, causing sunburn more prominently than UVA radiation [8]. Previous studies suggest that UVB exposure leads to the generation of ROS within cells, triggering the activation of the mitogen-activated protein kinase (MAPK) signaling pathway [9], which, in turn, increases the expression of matrix metalloproteinases (MMPs), resulting in the degradation of collagen and lipids in the skin and the manifestation of aging-related characteristics (i.e., skin aging phenotypes) [10–12]. Additionally, UVB radiation can induce DNA damage and expedite skin aging by activating internal aging factors [13–15], and N6-methyladenosine (m^6A) methylation has been reported to play a unique role in repairing critical DNA segments [16–18]. However, the precise regulation of m^6A methylation during the aging process remains to be elucidated.

m^6A modification refers to the addition of a methyl group to the nitrogen-6 position of adenosine nucleotides [19]. This modification is the most prevalent internal alteration found in mammalian cells' mRNA and plays a critical role in regulating various processes, such as precursor mRNA maturation, translation, and degradation, which are associated with different disorders [20,21]. Three primary proteins are involved in m^6A modifications: methyltransferases, demethylases, and proteins that specifically recognize m^6A-methylated transcripts [22–25]. Some studies have reported that METTL3 and METTL14 methylation may be involved in repairing DNA damage caused by UV radiation [26]. Additionally, it has been demonstrated that METTL3 regulates global genome repair and protects against UVB-induced photoaging through selective autophagy. Moreover, the m^6A-modified RNA profile can be influenced by advanced glycosylation end products and METTL14 overexpression in UVB-induced photoaging human dermal fibroblasts, further promote fibroblast proliferation. These findings suggest that METTL3 and METTL14 may have complex regulatory effects on UVB-induced photoaging depending on specific circumstances [27].

To further explore the pathogenesis of photoaging, we conducted a comprehensive whole-transcriptome analysis to identify the mRNA and long noncoding RNA (lncRNA) molecules that exhibit differential expression in photoaged skin compared to normal skin. Our findings highlight the significantly elevated levels of METTL3 and METTL14 in photoaged skin, and we conducted follow-up *in vitro* and *in vivo* experiments to determine and validate the roles of the identified genes and pathways in photoaging pathogenesis.

2. Materials and methods

2.1. Patient samples

Skin tissue samples were collected from both The normal and photoaging patients at the Third Affiliated Hospital of Central South University, following approval by the Hospital Institutional Review Board. The skin specimens were obtained from two distinct areas: sun-protected regions (15 cases from the back or buttocks) and sun-exposed regions (15 cases from the face) of subjects with normal areas surrounding benign lesions.

2.2. Cell culture and UVB-induced photoaging model

HaCaT and Primary keratinocytes, obtained from the ATCC (Type Culture Collection) in the USA and certified, were cultured in Dulbecco's Modified Eagle Medium (Corning, USA) supplemented with 15 % fetal bovine serum (Gibco, USA) and antibiotics (Gibco, USA). To simulate UVB radiation exposure, keratinocytes were subjected to varying intensities of UVB radiation (range, 0–120 mJ/cm^2) three times within a 72-h timeframe, and the optimal exposure intensity was determined.

2.3. UVB-induced photoaged mouse modelell culture

The minimum erythema dose (MED) was determined using the following procedure: Eight Balb/c mice were selected, and the hair on their backs was shaved. Four different irradiation time points were established, consisting of 10 min, 15 min, 20 min, and 30 min, with two mice assigned to each time point. On the second day, mice exposed to 10 or 15 min of irradiation did not exhibit noticeable erythema, whereas those exposed to 30 min showed evident erythema. Therefore, an irradiation time of 30 min was selected as the MED. The calculation of the MED was performed as follows: 1 MED = (0.134 μW/cm^2) × 30 min = 4.02 mJ/cm^2, with an irradiation height of 30 cm. Based on preliminary experiments, the mice underwent an adaptive feeding period and were exposed to 1 MED for eight weeks.

2.4. SAH-induced mouse model

SAH is an inhibitor for METTL3-METTL14 heterodimer complex (METTL3-14) with an IC50 of 0.9 μM. Balb/c mice back hairs was shaved and then injected with SAH (5 μM) 1 time for 2 weeks. Collected their skins and detected METTL3 and METTL14 levels to convince the SAH-induced mouse model was constructed successfully.

2.5. Small interfering (si) RNA and adenovirus transfection of cells

Keratinocytes were seeded onto 6 cm dishes at a density of 1 × 106 cells and incubated in a medium containing 10 % fetal bovine serum. The cells were then treated with siMETTL3, siMETTL14, AAV-METTL3 and AAV-METTL14 for 48 h, following which images of the cells were captured using a Zeiss LSM710 confocal microscope system (Carl Zeiss, Oberkochen, Germany), and image analysis was performed using Adobe Photoshop R@ZEN Lite 2012 (Adobe Systems, CA, USA).

2.6. Quantification of global m^{6}A levels

The EpiQuikTM m6A RNA Methylation Quantification Kit (colorimetric method; EpigenTek, NY, USA) was used according to the manufacturer's protocol. Briefly, 200 ng of RNA isolated from skin tissues was applied to different assay wells. Subsequently, the capture antibody solution, detection anti-m6A antibody solution, and enhancer solution were sequentially added to the detection wells at appropriate dilution concentrations. The levels of m6A were quantified by measuring the absorbance of each well at 450 nm and calculating the values based on a standard curve. All experiments were repeated three times.

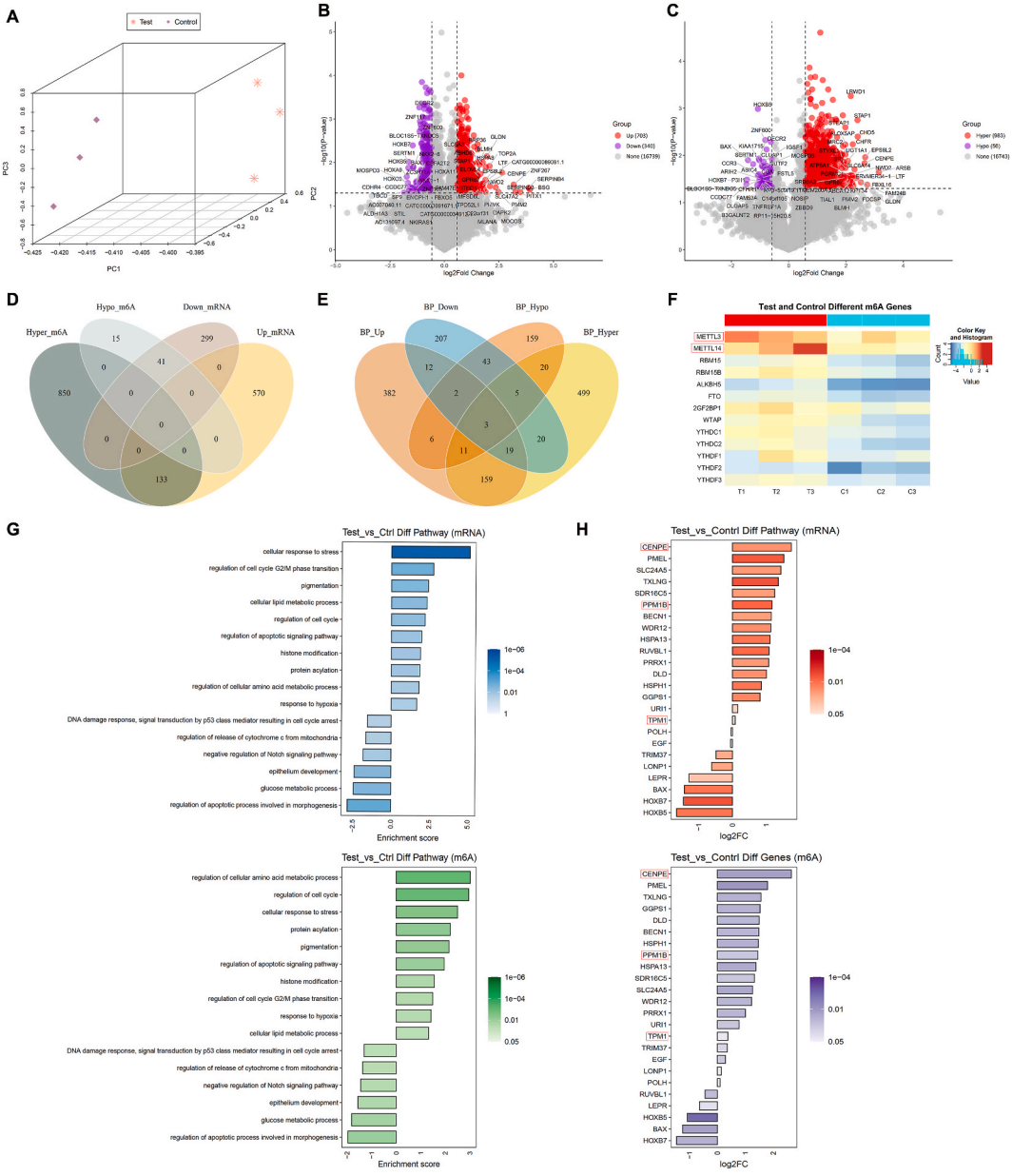

Fig. 1. Epitope transcription microarray analysis of mRNAs and m^{6}A-mRNAs in photoaging. (**A**) Principal component analysis (PCA) plot showing significant methylation differences between sun-protected and sun-exposed skins (n = 3). (**B, C**) Volcano plot showing the differentially expressed mRNAs and m^{6}A-mRNAs between sun-protected and sun-exposed skins (upregulation: red; downregulation: purple). (**D, E, F**) Venn diagram showing the overlap of differentially expressed genes (DEGs), m^{6}A-modified genes, biological processes (BPs), and the hsa pathways between sun-exposed and non-exposed skins. (**G**) Enrichment analysis of 16 pathways involved by GO and KEGG. (**H**) Enrichment analysis of DEGs and m^{6}A-modified genes involved by GO and KEGG. GO: Gene Ontology; KEGG: Kyoto Encyclopedia of Genes and Genomes. P values are indicated by different colors. The significance was defined by Fold change $\geq$2, FDR $<$0.05 and P $<$ 0.05.

2.7. Methylated RNA immunoprecipitation (MeRIP)-qPCR

To isolate 40 μg of total RNA was used for IP with an anti-m6A antibody. Briefly, 300 μL of IP buffer was added to a mixture of total RNA and m6A pegged controls, followed by incubation at 4 °C for 2 h. The mixture was then washed and incubated with sheep anti-rabbit IgG. Afterward, three washes with wash buffer for 1 h. Finally, the enriched RNA was purified using the RNeasy Mini Kit (Qiagen, MD, USA) for subsequent analysis. To validate the data obtained from the microarray analysis, the IP-RNA from the samples (with a ratio of 3:3 between the control group and experimental group) was subjected to MeRIP-qPCR using real-time fluorescence quantitative polymerase chain reaction.

2.8. m^6A-mRNA & lncRNA Epitranscriptomic microarray analysis and bioinformatics analysis

Microarray hybridization was performed following the standard protocol provided by ArrayStar. Briefly, the cRNAs were labeled with cy5, then fragmented before being hybridized to transcribed microarrays (860K, Arraystar) specifically designed for human m^6A-mRNA and lncRNA analysis. Following the hybridization process, the slides were rinsed, and the hybridization arrays were scanned using an Agilent G2505C scanner (Agilent, Beijing, China) in a two-color channel, and the data were analyzed using Agilent feature extraction software (version 11.0.1.1). To identify differentially methylated m^6A RNA between the two groups, a fold-change threshold of $\geq$2 and a p-value threshold of $<$0.05 were used. All microarray analyses were conducted by Kangchen Biotechnology (Shanghai, China). The differentially expressed m6A-methylated mRNA transcription products were assigned to various Gene Ontology (GO) databases (http://geneontology.org/). Additionally, the Kyoto Encyclopedia of Genes and Genomes (KEGG) database

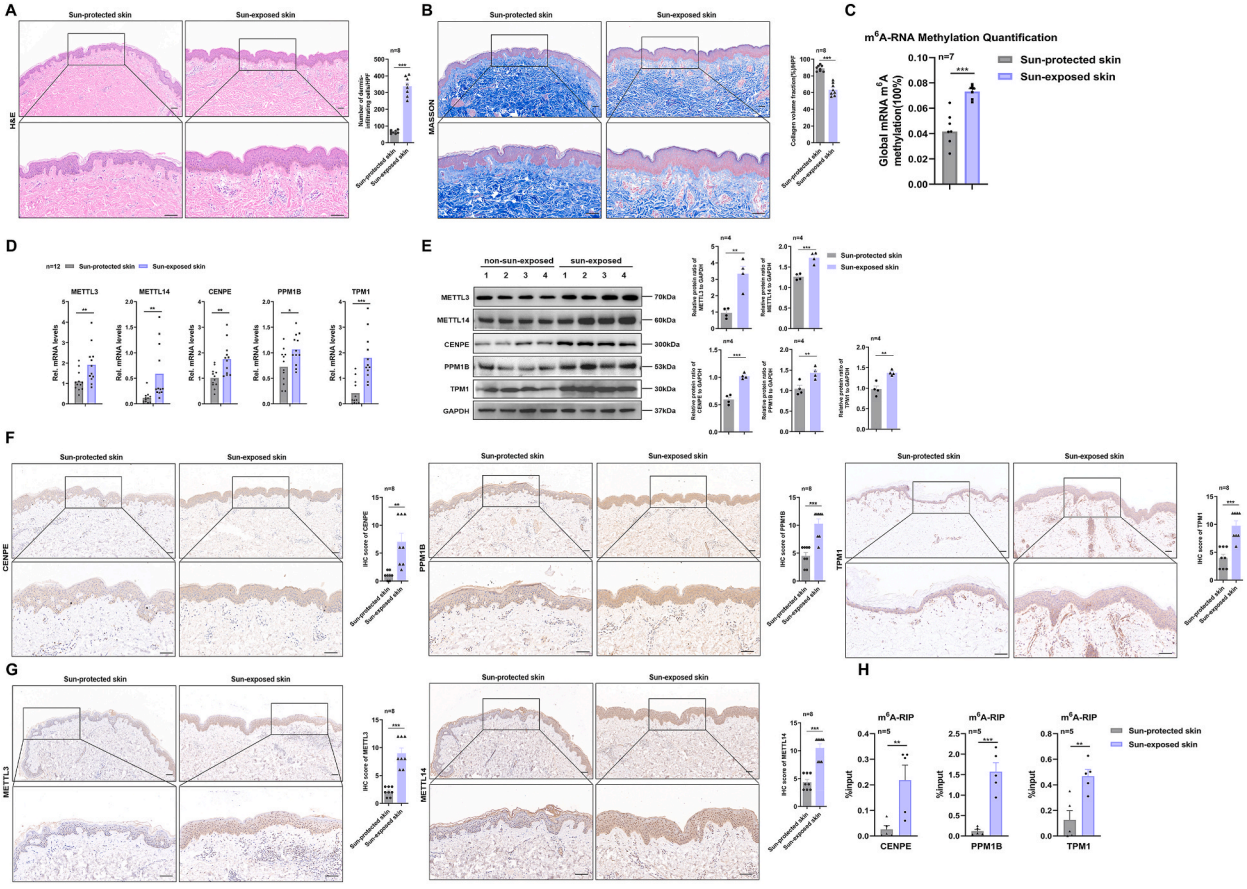

Fig. 2. The m^6A levels and m^6A-related DEGs elevated by UVB induced *in vitro*. (**A**) Schematic diagram of the overall design process of the experiment. (**B**) Representative image of β-Gal staining of control and UVB-photoaged Primary cells. (**C**) Representative image of ROS fluorescence staining of control and UVB-photoaged Primary cells. (**D**) The mRNA expression levels of SASP factors (P16, P21, IL-6, IL-1β, TNF-α and VEGF) in control and UVB-photoaged Primary cells (n = 6). (**E**) The global level of m^6A and m^6A modification enzymes mRNA levels in control and UVB-photoaged Primary cells (n = 5). (**F**) qPCR analysis of m^6A-related genes in control and UVB-photoaged Primary cells (n = 3). (**G**) Immunoblot analysis of the indicated proteins (METTL3, METTL14, CENPE, PPM1B and TPM1) in control and UVB-photoaged Primary cells (n = 3). Gray values (measured by Image J) indicate significant differences. (**H**) MeRIP-qPCR analysis showing the m^6A modification levels of three indicated DEGs (CENPE, PPM1B and TPM1) in control and UVB-photoaged Primary cells (n = 5). *P < 0.05; **P < 0.01; ***P < 0.001.

(https://www.kegg.jp/) was used to further analyze the functional pathways associated with these mRNAs.

2.9. Statistical analysis

The results are representative of at least three independent experiments. The significance of the microarray analysis and MeRIP-qPCR results was assessed using Student's t-test. Fisher's exact test was utilized to determine the significance of the GO and KEGG analyses. All data are expressed as means ± standard deviations. Statistically significant p-values were set at < 0.05.

3. Results

3.1. m6A modification profiles of mRNAs in sun-protected and sun-exposed skin tissues

We performed a transcriptional microarray study on mRNA and lncRNA to identify specific m^{6}A methylation modifications in photoaged skin. By analyzing the m^{6}A modification profiles of three pairs of healthy human sun-protected and sun-exposed skin tissues, we identified a total of 42,993 transcripts, including 34,906 mRNAs and 8087 lncRNAs (Figs. S1A and B). Hierarchical clustering analysis revealed significant expression pattern differences between the sun-protected and sun-exposed regions (Fig. 1A). We further screened genes with significant changes (fold change ≥2) and found that 340 (1.91 %) mRNA genes were downregulated and 703 (3.95 %) mRNA genes were upregulated (Fig. 1B). In addition, 983 (5.52 %) genes were hypermethylated, and 56 (0.31 %) genes were hypomethylated (Fig. 1C). Association analysis of mRNAs and m^{6}A-mRNAs was performed on the differentially expressed

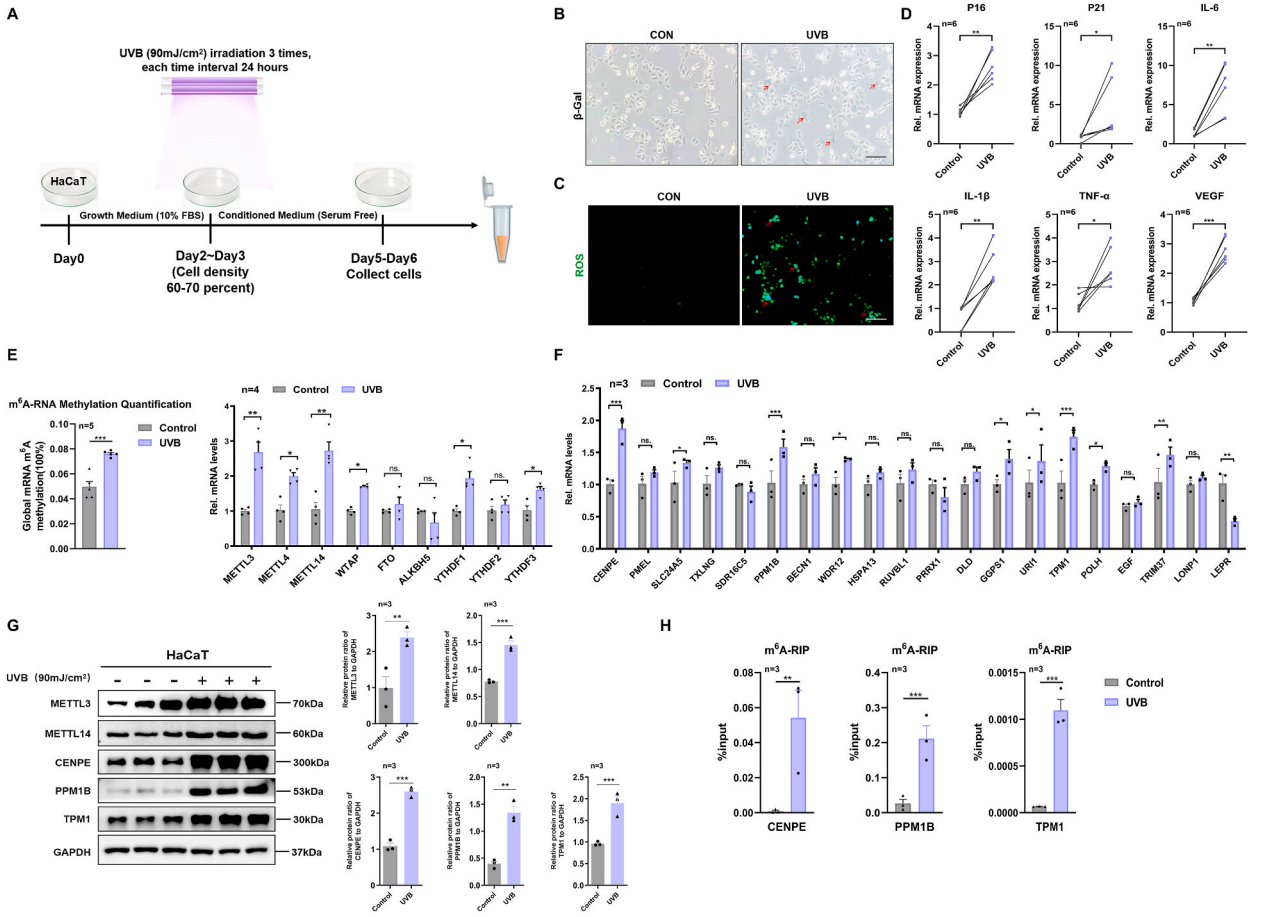

Fig. 3. The m^{6}A levels and three indicated DEGs increased in sun-exposed skin tissues. (**A, B**) HE and Masson staining analysis of sun-protected and sun-exposed skin tissues (n = 8). (**C**) The global level of m^{6}A in sun-protected and sun-exposed skin tissues (n = 7). (**D**) The mRNA expression levels of METTL3, METTL14, CENPE, PPM1B and TPM1 in sun-protected and sun-exposed skin tissues (n = 12). (**E**) Immunoblot analysis of METTL3, METTL14, CENPE, PPM1B and TPM1 in sun-protected and sun-exposed skin tissues (n = 8). Gray values (measured by Image J) indicate significant differences. (**F, G**) Immunohistochemical staining of METTL3, METTL14, CENPE, PPM1B and TPM1 in sun-protected and sun-exposed skin tissues (n = 8). (**H**) MeRIP-qPCR analysis showing the m^{6}A modification levels of CENPE, PPM1B and TPM1 in sun-protected and sun-exposed skin tissues (n = 5). Scale bar = 50 μm. The data represent means ± SEMs. *P < 0.05; **P < 0.01; ***P < 0.001.

genes, revealing that 133 (6.97 %) genes exhibited upregulated mRNA expression accompanied by m^{6}A hypermethylation, while 41 (2.15 %) genes displayed downregulated mRNA expression and m^{6}A hypermethylation simultaneously (Fig. 1D). Furthermore, we identified 43 (2.78 %) biological processes (BP) that showed simultaneous m^{6}A hypermethylation modification (BP-Hypo) and downregulation of mRNA expression (BP-Down), as well as 159 (10.28 %) BP pathways that exhibited simultaneous m^{6}A hypermethylation modification (BP-Hyper) (Fig. 1E and F). KEGG pathway enrichment analysis revealed that mRNAs with high m^{6}A methylation levels were primarily associated with the "cellular response to stress" and "regulation of cell cycle G2/M phase transition" pathways, while mRNAs with low m^{6}A levels were mainly involved in the "regulation of apoptotic process" and "glucose metabolic process" pathways (Fig. 1G). Notably, the top 19 differentially elevated mRNAs and m^{6}A -mRNAs, as well as the top 5 downregulated mRNAs and m^{6}A-mRNAs, were identified (Fig. 1H–S1C, D). Overall, these findings strongly suggest that increased methylation levels and m^{6}A modification of mRNAs have an impact on skin photoaging.

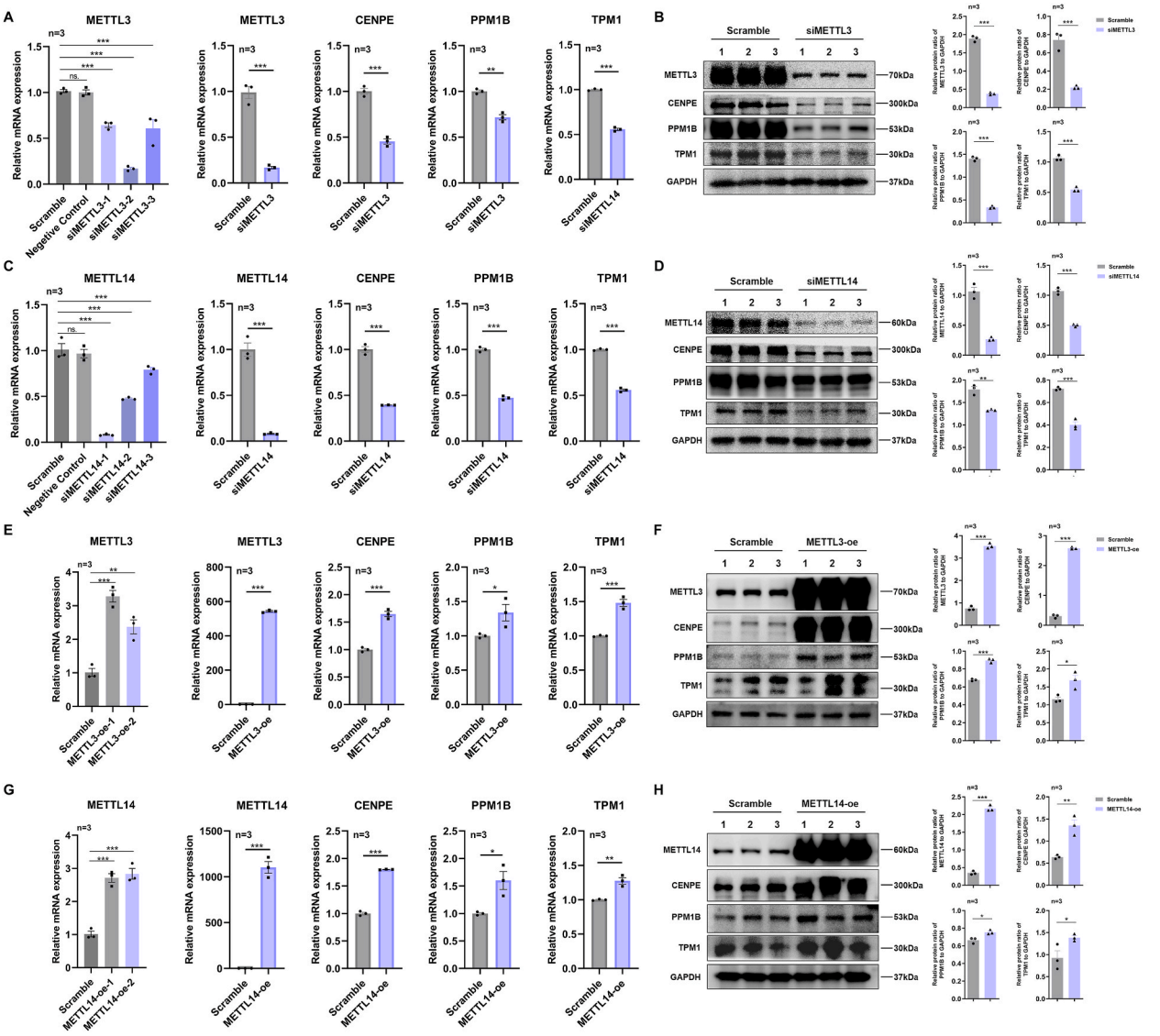

Fig. 4. Validation of three indicated DEGs expression in primary keratinocytes after intervening with the expression of METTL3 **and** METTL14. (**A, B**) qPCR and immunoblot analysis of METTL3, CENPE, PPM1B and TPM1 expression levels in primary keratinocytes post knockdown of METTL3. (**C, D**) qPCR and immunoblot analysis of METTL14, CENPE, PPM1B and TPM1 expression levels in primary keratinocytes with knockdown of METTL14. (**E, F**) qPCR and immunoblot analysis of METTL3, CENPE, PPM1B and TPM1 expression levels in primary keratinocytes post overexpressed METTL3. (**G, H**) qPCR and immunoblot analysis of METTL14, CENPE, PPM1B and TPM1 expression levels in primary keratinocytes with overexpressed METTL14. Gray values (measured by Image J) indicate significant differences. The data represent means ± SEMs. *P < 0.05; **P < 0.01; ***P < 0.001.

3.2. METTL3 and METTL14 overexpression induced m6A modification of CENPE, PPM1B, and TPM1 in vitro

In this study, we utilized UVB-induced HaCaT keratinocytes to investigate the impact of differentially expressed genes (DEGs) during photoaging *in* an *in vitro* setting (Fig. 2A). Firstly, we observed that UVB-treated HaCaT keratinocytes exhibited senescence, as indicated by β-galactosidase staining and higher levels of intracellular reactive oxygen species (ROS) compared to the control group (Fig. 2B and C). The increased expression of P16 and P21, along with elevated levels of senescence-associated secretory phenotypes (SASP) such as IL-6, IL-1β, and TNF-α, further confirmed the aging phenotype of UVB-induced photoaging cells (Fig. 2D). Additionally, we observed a higher global level of m^6A modification and significantly increased expression levels of METTL3 and METTL14 in UVB-induced cells compared to control cells (Fig. 2E). This led us to hypothesize that the elevated m^6A levels of DEGs in photoaging may be attributed to the upregulation of the m^6A methyltransferases METTL3 and METTL14. Moreover, the mRNA expression levels of CENPE, PPM1B and TPM1, which are known as m^6A-modified DEGs, were significantly elevated in the photoaging group (Fig. 2F), suggesting their involvement in photoaging. Subsequently, we confirmed that the protein levels of the two m^6A methyltransferases, METTL3 and METTL14, as well as the three indicated m^6A-modified DEGs, CENPE, PPM1B, and TPM1, were upregulated in UVB-induced photoaging cells compared to the control group (Fig. 2G). Furthermore, MeRIP-qPCR analysis performed on UVB-induced HaCaT cells revealed significant regulation of m^6A levels in CENPE, PPM1B, and TPM1 (Fig. 2H). Taken together, the findings suggest that UVB exposure leads to the upregulation of METTL3, METTL14, and three DEGs, resulting in increased overall m^6A methylation levels and elevated m^6A levels, specifically in CENPE, PPM1B and TPM1.

3.3. Identification of METTL3 and METTL14 mediated m6A modification of CENPE, PPM1B, and TPM1 in sun-exposed skin tissues

To further validate the findings on the changes in METTL3, METTL14, CENPE, PPM1B and TPM1, we performed additional experiments using sun-protected and sun-exposed skin samples obtained from 12 pairs of age-matched human subjects. Histological analysis through HE and Masson staining revealed a significant increase in inflammatory cells, particularly neutrophils, in sun-exposed skins compared to sun-protected skins (Fig. 3A). Additionally, collagen synthesis was reduced, and structural disruptions were observed in sun-exposed skins, indicating signs of photoaging (Fig. 3B). Moreover, we found that the overall m^6A levels were upregulated in sun-exposed skins compared to sun-protected skins (Fig. 3C). Furthermore, the expression levels of METTL3, METTL14, CENPE, PPM1B, and TPM1 were significantly elevated in sun-exposed skins compared to sun-protected skins (Fig. 3D and E).

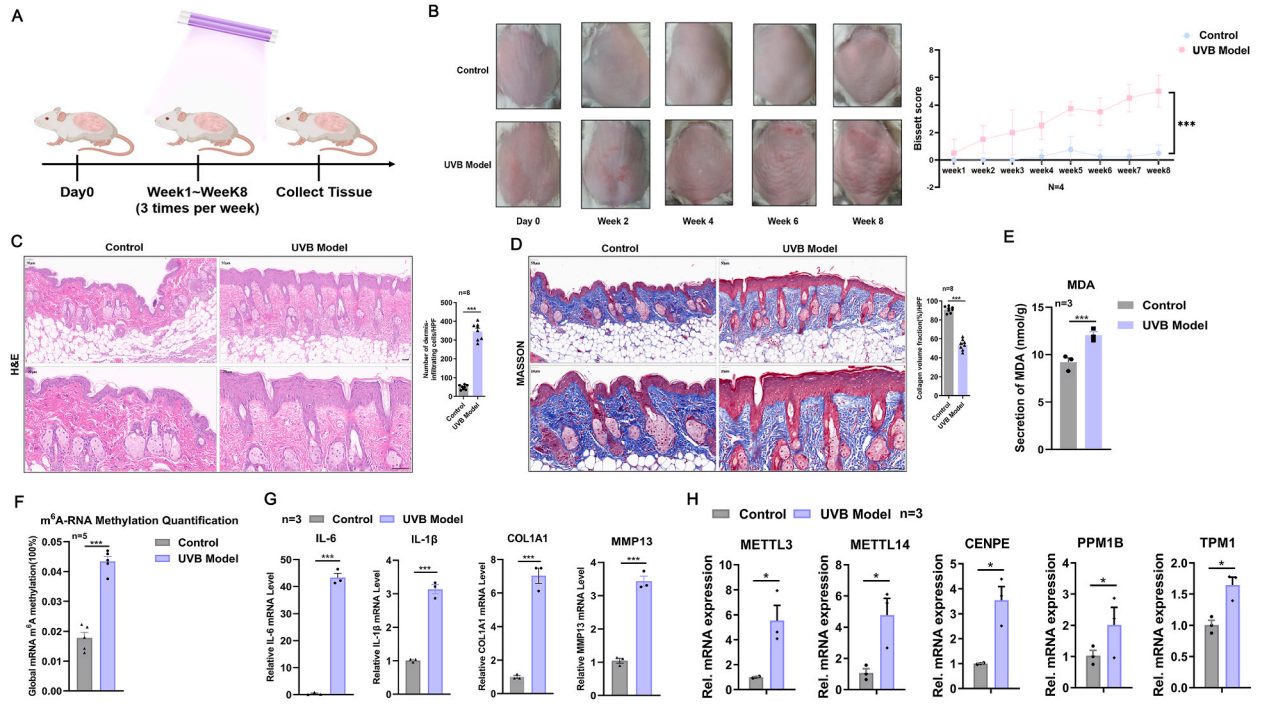

Fig. 5. Validation of METTL3, METTL14 **and three indicated DEGs expression *in vivo*.** (**A**) Schematic diagram of UVB-induced photoaging model mice. (**B**) Observation of back skin and skin macroscopic score in the control group and the model group at 0, 2, 4, 6 and 8 weeks after modeling. (**C, D**) HE and Masson staining analysis of control and model group skin tissues (n = 8). (**E**) ELISA analysis of MDA levels in control and model group skin tissues. (**F**) The global level of m^6A in the skin tissues (n = 3) of the control and the model group. (**G**) qPCR analysis of IL-6, IL-1β, COL1A1 and MMP13 mRNA levels in the skin tissues (n = 3) of the control and the model group. (**H**) qPCR analysis of METTL3, METTL14, CENPE, PPM1B and TPM1 expression levels in the skin tissues (n = 3) of the control and the model group. The data represent means± SEMs. *P < 0.05; **P < 0.01; ***P < 0.001.

Immunohistochemistry staining confirmed the higher expression levels of METTL3, METTL14, CENPE, PPM1B, and TPM1 in sun-exposed skins compared to sun-protected skins, supporting that significant positive correlations between the increased expression of METTL3 and METTL14 and higher expression levels of CENPE, PPM1B, and TPM1 in sun-exposed samples (Fig. 3F and G). Additionally, the m^6A levels of CENPE, PPM1B, and TPM1 were also found to be upregulated in sun-exposed skins (Fig. 3H). Collectively, these findings support the notion that the elevated expression of METTL3 and METTL14 mediates higher m^6A modification in sun-exposed skins, leading to increased expression of CENPE, PPM1B, and TPM1, which are implicated in photoaging.

3.4. UVB-induced photoaging depends on METTL3 and METTL14 m6A modified three indicated DEGs

To confirm the causal role of METTL3 and METTL14 in regulating the expression of the three candidate DEGs in photoaging, we employed siRNA knockdown of METTL3 and METTL14, as well as adeno-associated virus (AAV) overexpression of METTL3 and METTL14 in primary keratinocytes (Fig. S2A). Initially, we screened for small RNA sequences and viruses with the most effective knockdown and overexpression effects. Subsequently, we observed significant downregulation of CENPE, PPM1B and TPM1 expression in primary keratinocytes with stable knockdown of METTL3 (Fig. 4A and B). Similarly, the knockdown of METTL14 also led to a significant reduction in the expression of CENPE, PPM1B and TPM1 (Fig. 4C and D). Conversely, the overexpression of METTL3 and METTL14 substantially increased the expression of CENPE, PPM1B and TPM1 in primary keratinocytes (Fig. 4E, F, G, H). These

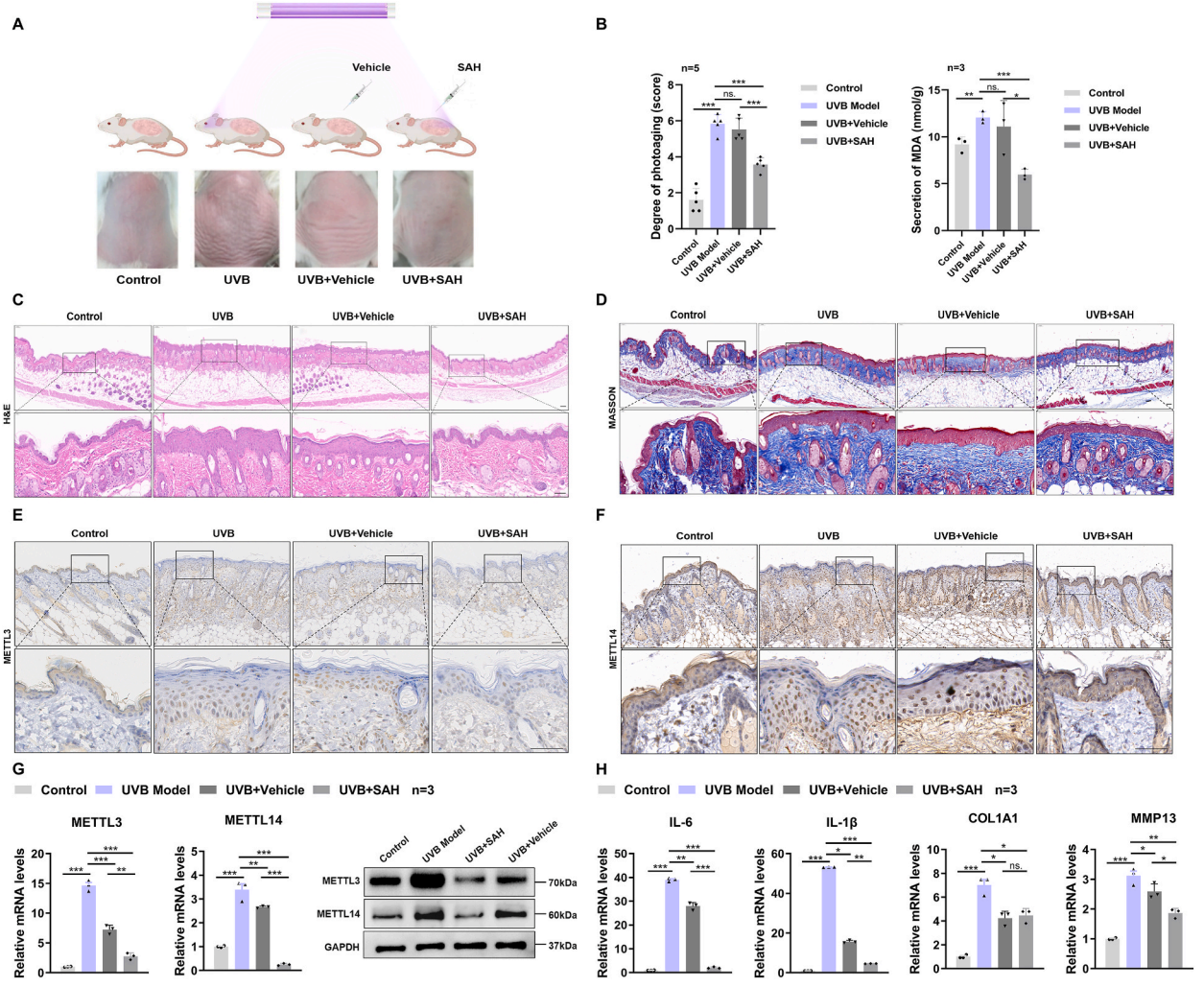

Fig. 6. Validation of METTL3 and METTL14 mediated three indicated DEGs methylation facilitates UVB-induced photoaging. (A) Schematic diagram and phenotypic changes of back lesions in UVB-induced photoaging model mice treated with SAH (METTL3 and METTL14 inhibitor). (**B**) Skin macroscopic score and MDA levels in mice groups after modeling. Dermal infiltrating cells and the dermal collagen volume fraction are quantified by Image J. (**C, D**) HE and Masson staining analysis of mice skin tissues. (**E, F**) Immunohistochemical staining of METTL3 and METTL14 in mice skin tissues. (**G**) qPCR and immunoblot analysis of METTL3 and METTL14 expression levels. (**H**) qPCR analysis of IL-6, IL-1β, COL1A1, and MMP13 mRNA levels in mice skin tissues (n = 3). The data represent means± SEMs. *P < 0.05; **P < 0.01; ***P < 0.001.

findings suggest that the depletion of METTL3 and METTL14 results in downregulating CENPE, PPM1B and TPM1 expression and reduced methylation of CENPE, PPM1B, and TPM1. This supports the mechanism whereby the CENPE, PPM1B, and TPM1 genes may function as downstream targets of METTL3 and METTL14-mediated m^{6}A modifications, contributing to the initiation and progression of UVB-induced photoaging.

3.5. METTL3 and METTL14 regulate the m^{6}A modification of three candidate DEGs in vivo

Next, we investigated the *in vivo* changes in m^{6}A methylation genes in mice subjected to UVB-induced photoaging (Fig. 5A). Compared to the control group, the mice in the model group exhibited noticeable wrinkles, irregular thickening, and pigmentation on their back skin after eight weeks. Photoaging scoring confirmed a significant increase in the score of the UVB model group (Fig. 5B). HE staining revealed characteristic features of photoaging skin in the model group, including excessive keratosis of the stratum corneum, irregular thickening of the epidermis, and significant infiltration of inflammatory cells in the dermis, as opposed to healthy skin (Fig. 5C). Furthermore, Masson staining demonstrated a decrease in the content of collagen fibers in the dermis of the UVB model group, with an irregular arrangement and the presence of broken and sparse fibers (Fig. 5D). Additionally, we measured the levels of malondialdehyde (MDA), a lipid peroxide product associated with aging, which significantly increased in the UVB-induced photoaging mouse model, indicating the successful induction of the photoaging phenotype (Fig. 5E). Furthermore, we observed a greater increase in the global m^{6}A level in the skin of the UVB mouse model compared to the control group (Fig. 5F). Based on the photoaging standard, the model group exhibited significantly higher levels of IL-1β, IL-6, COL1A1 and MMP13 than the control group (Fig. 5G). Moreover, we observed the mRNA expression levels of METTL3, METTL14, CENPE, PPM1B and TPM1 significant increase in following UVB treatment (Fig. 5H). These findings suggest that m^{6}A-related modifying enzymes are upregulated to varying degrees in the skin of the photoaging model mice.

3.6. METTL3 and METTL14 mediated three indicated DEGs methylation facilitates UVB-induced photoaging

To investigate whether METTL3 and METTL14 can affect the m^{6}A modification of the three candidate DEGs, we subcutaneously injected SAH (a METTL3 and METTL14 inhibitor) into the UVB-induced photoaging model mice. The macroscopic appearance of the back skin in each group of mice is shown in the figure (Fig. 6A). Compared to the control group, the UVB group displayed typical skin photoaging features, including wrinkles, erythema, edema, and pigmentation. However, the SAH group exhibited a significant reduction in wrinkles and improved color sedimentation compared to the UVB group. The content of MDA significantly increased in the UVB group, and there was a slight elevation in the UVB + SAH group compared to the UVB + Vehicle group (Fig. 6B). HE sections revealed a significant decrease in epidermal thickness in the UVB + SAH group compared to the UVB group and the UVB + Vehicle group (Fig. 6C). Masson staining showed fewer collagen fiber breaks and reduced infiltration of inflammatory cells in the UVB + SAH group compared to the UVB + Vehicle group (Fig. 6D). Moreover, IHC analysis demonstrated that the expression of METTL3 and METTL14 significantly increased in the UVB model group and UVB + Vehicle group compared to the control group, while it was lower in the UVB + SAH group (Fig. 6E and F). Consistently, we confirmed that the mRNA and protein expression levels of METTL3 and METTL14 were significantly higher in the UVB + Vehicle group and the UVB model group compared to the control group, while they were lower in the UVB + SAH group (Fig. 6G). The mRNA expression levels of IL-6, IL-1β, COL1A1, and MMP13 increased in the UVB model group and UVB + Vehicle group after UVB induction and significantly decreased in the UVB + SAH group following UVB + SAH intervention (Fig. 6H). In summary, these findings demonstrate that the genes regulated by the m^{6}A methyltransferases METTL3 and METTL14 play a role in the initiation and progression of UVB-induced photoaging.

4. Discussion

Photoaging is a harmful skin condition caused by prolonged exposure to external ultraviolet radiation. Apart from visible signs of aging like wrinkles and pigmentation, it also compromises the skin's protective barrier, increases susceptibility to infections, and even raises the risk of skin cancer [28]. The early pathological changes in photoaging involve DNA damage, inflammatory responses, increased production of ROS and enhanced secretion of senescence-associated secretory phenotypes (SASP), resulting in premature senescence of major skin cells [29,30]. Senescent cells release molecules associated with aging, including IL-6 and TNF-α, which further accelerate skin aging [31,32]. Recently, m^{6}A, the most prevalent posttranscriptional mRNA modification in eukaryotes, has emerged as a significant regulator of aging [33]. Therefore, we aimed to investigate the expression patterns of m^{6}A regulatory molecules in photoaging and explore the methylation modification pathways that contribute to the distinct epigenetics of photoaging. Our findings indicate that METTL3 and METTL14 levels increase and m6A total methylation levels are up-regulated, which can regulate the hypermethylation modification of the mRNA of CENPE, PPM1B and TPM1 molecules, thus promoting the inflammatory pathway related to cell aging and positively regulating the initiation and progression of photoaging.

The molecular and cellular mechanisms underlying UVB-induced photoaging are diverse. Several studies have highlighted the involvement of epigenetic changes in aging processes across different systems. For instance, the impact of m^{6}A modification on AGO2 mRNA levels during human aging has been observed to regulate the expression of aging-related miRNAs [34]. It has also been demonstrated that UV exposure leads to increased m^{6}A mRNA levels and localization at DNA damage sites, and this process is positively regulated by METTL3 and METTL14 [18]. AGEs have been shown to elevate overall m^{6}A modification levels in photodamaged skin *in vivo* and in skin fibroblasts *in vitro* [35]. In line with these findings, our study through sequencing of exposed and non-exposed skin tissues, UVB-induced photoaging cell models, and cellular molecular biological methods, we found that the

expression of METTL3 and METTL14 was upregulated and the hypermethylated genes CENPE, PPM1B, TPM1 and pathway were upregulated in exposed skin tissues. Overexpression of METTL3 and METTL14 significantly increased the expression of CENPE, PPM1B, TPM1 and senescence related secretory molecules in UVB-induced KC cells. These results indicated that METTL3 and METTL14 could regulate the m^6A modification of CENPE, PPM1B and TPM1 to promote the photoaging phenotype induced by UVB. This reveals that the upregulation of METTL3 and METTL14 in UVB-induced photoaging promotes the high expression of CENPE, PPM1B and TPM1 and the accumulation of m^6A mRNA levels, which subsequently contributes to the release of aging-related secretory molecules and accelerates the skin photoaging process.

CENPE is a microtubule kinesin protein involved in cell cycle regulation [36]. It has been observed that CENPE DNA methylation is upregulated in certain cancers, and inhibiting its expression can regulate transcription and promote tumor cell growth [37]. PPM1B is a member of the PP2C family of serine/threonine protein phosphatases involved in cell cycle regulation through the dephosphorylation of cyclin-dependent kinases (CDKs) [38]. The overexpression of PPM1B can induce cell growth arrest or apoptosis, and it is known to be involved in cellular senescence [39]. PPM1B has been shown to control senescence and cell proliferation in public databases [40]. TPM1 is an actin-binding protein associated with cellular senescence and inflammatory responses [41], which can promote the LPS-induced microglial inflammatory response and peripheral neuronal death via the PKA/CREB pathway [42]. According to our study, the expression and methylation of CENPE, PPM1B, and TPM1 were highly coexpressed in UVB-induced photoaging cells and sun-exposed skins, indicating that these enzymes may be involved in the pathological modifications associated with photoaging. The increase in transcription of CENPE, PPM1B, and TPM1 induced by m^6A methylation suggests their potential involvement in the onset and progression of photoaging.

In vivo experiment, we inhibited the expression of METTL3 and METTL14 in the epidermis of mice by SAH (METTL3 and METTL14 inhibitors), and found that after UVB irradiation, the skin wrinkles, erythema, edema and pigmentation of mice in SAH group were significantly reduced. Additionally, the SAH-treated group had a thinner epidermis and more organized collagen fiber bundles compared to the photoaging model group. SAH administration effectively delayed the progression of skin photoaging, promoting the repair of skin structure and regeneration of collagen fibers. SAH injection resulted in reduced expression of inflammation factors IL-6, IL-1β, COL1A1, and MMP13 mRNA, as well as decreased levels of MDA in the photoaging skin, indicating that SAH inhibited the aging process. Moreover, SAH treatment decreased the expression of m^6A modifying enzymes METTL3 and METTL14, along with related markers in the UVB-induced model, resulting in lower m^6A levels and suppression of photoaging. Thus, our findings indicate that inhibition of METTL3 and METTL14 can regulate the m^6A modification of photoaging related molecules and delay the UVB-induced skin photoaging phenotype.

In our analysis, external UVB up-regulated the expression of METTL3 and METTL14 in the skin, thus promoting the hypermethylation of CENPE, PPM1B and TPM1, activating the cellular inflammatory pathway and cell aging, resulting in skin photoaging. However, the specific regulatory mechanisms of how METTL3 and METTL14 are added or removed from mRNA and how to regulate the specific target of mRNA still need to be further studied. The follow-up demonstration can be carried out in gene knockout mice with low expression of METTL3 and METTL14 in the epidermis of photoaging mice to further demonstrate our results. In addition, the sequencing results showed that 133 mRNA expressions of differentially expressed genes in exposed skin were up-regulated and m6A hypermethylated, 41 mRNA expressions were down-regulated and m^6A hypomethylated, and 159 BP pathways showed m^6A hypermethylated modification. We can further study the differentially expressed genes and pathways to find other potential therapeutic targets.

Our study highlights the important role of m^6A methylation in regulating gene expression in UVB-induced photoaging. We found that the upregulation of METTL3 and METTL14 in UVB-induced photoaging cells and sun-exposed skin tissues contribute to the upregulation of CENPE, PPM1B and TPM1 expression through m^6A methylation, which may promote the development of photoaging. Targeting METTL3 and METTL14, m^6A methylation modifications of CENPE, PPM1B and TPM1 in keratinocytes and fibroblasts can be reduced, thereby reducing the expression of aging related molecules and inflammatory factors, and slowing down the UVB-induced cellular aging process. It is a promising strategy for preventing and treating UVB-induced photoaging. Further investigations are warranted to validate these findings and elucidate the underlying mechanisms.

5. Conclusions (4–5 lines - Optional)

In summary, our study sheds light on the molecular pathways and signatures involved in the development of age-related phenotypes, with a specific focus on the role of RNAs methylation in photoaging, findings RNAs m^6A modification facilitates UVB-induced photoaging, which has broad implications for the diagnosis and targeted treatment of photoaging and the improvement of the aging state.

Ethical approval statement

Ethics approval was granted by The IRB of Third Xiangya Hospital Ethics Committee (No. 2022-S171) and the Institutional Experimental Animal Committee of Central South University (No.XMSB-2022-0167).

CRediT authorship contribution statement

Shuping Zhang: Writing – original draft, Software, Methodology, Conceptualization. **Meng Wu:** Data curation. **Tingting Lu:** Visualization. **Xiaoying Tian:** Visualization. **Lihua Gao:** Investigation. **Siyu Yan:** Supervision. **Dan Wang:** Software. **Jinrong Zeng:**

Validation. **Lina Tan:** Writing – review & editing.

Data availability statement

Data associated with study not been deposited into a publicly available repository. Data will be made available on request.

Funding

This work was supported by grants from the Wisdom Accumulation and Talent Cultivation Project of The Third Xiangya Hospital of Central South University (No. YX202214), the National Natural Science Foundation of China (No. 82273508) and China Postdoctoral Science Foundation funded project (No. 2022M713537).

Declaration of competing interest

The authors declare that they have no known competing financial interests or personal relationships that could have appeared to influence the work reported in this paper.

Acknowledgements

We thank all individuals who participated in this work. We are grateful for all the funding provided by funded projects. Specially thanks to the support from Postdoctoral Station of Clinical Medicine, the Third Xiangya hospital, central south university.

Appendix A. Supplementary data

Supplementary data to this article can be found online at https://doi.org/10.1016/j.heliyon.2024.e39532.

References

[1] E. Bang, D.H. Kim, H.Y. Chung, Protease-activated receptor 2 induces ROS-mediated inflammation through Akt-mediated NF-kappaB and FoxO6 modulation during skin photoaging, Redox Biol. 44 (2021) 102022, https://doi.org/10.1016/j.redox.2021.102022.
[2] D.L. Sachs, J. Varani, H. Chubb, S.E.G. Fligiel, Y. Cui, K. Calderone, Y. Helfrich, G.J. Fisher, J.J. Voorhees, Atrophic and hypertrophic photoaging: Clinical, histologic, and molecular features of 2 distinct phenotypes of photoaged skin, J. Am. Acad. Dermatol. 81 (2019) 480–488, https://doi.org/10.1016/j.jaad.2019.03.081.
[3] J.H. Oh, Y.H. Joo, F. Karadeniz, J. Ko, C.S. Kong, Syringaresinol inhibits UVA-induced MMP-1 expression by suppression of MAPK/AP-1 signaling in HaCaT keratinocytes and human dermal fibroblasts, Int. J. Mol. Sci. 21 (2020), https://doi.org/10.3390/ijms21113981.
[4] Y.L. Vechtomova, T.A. Telegina, A.A. Buglak, M.S. Kritsky, UV radiation in DNA damage and repair involving DNA-photolyases and cryptochromes, Biomedicines 9 (2021), https://doi.org/10.3390/biomedicines9111564.
[5] M. Alam, R. Hughart, A. Champlain, A. Geisler, K. Paghdal, D. Whiting, J.A. Hammel, A. Maisel, M.J. Rapcan, D.P. West, E. Poon, Effect of platelet-rich plasma injection for rejuvenation of photoaged facial skin: a randomized clinical trial, JAMA Dermatol 154 (2018) 1447–1452, https://doi.org/10.1001/jamadermatol.2018.3977.
[6] K.C. Guerra, N. Zafar, J.S. Crane, Skin cancer prevention, StatPearls 87 (2022) 271–288, https://doi.org/10.1016/j.jaad.2022.01.053.
[7] D. Zargaran, F. Zoller, A. Zargaran, T. Weyrich, A. Mosahebi, Facial skin ageing: key concepts and overview of processes, Int. J. Cosmet. Sci. 44 (2022) 414–420, https://doi.org/10.1111/ics.12779.
[8] K. Tsuchida, M. Kobayashi, Ultraviolet A irradiation induces ultraweak photon emission with characteristic spectral patterns from biomolecules present in human skin, Sci. Rep. 10 (2020) 21667, https://doi.org/10.1038/s41598-020-78884-0.
[9] A. Salminen, K. Kaarniranta, A. Kauppinen, Age-related changes in AMPK activation: role for AMPK phosphatases and inhibitory phosphorylation by upstream signaling pathways, Ageing Res. Rev. 28 (2016) 15–26, https://doi.org/10.1016/j.arr.2016.04.003.
[10] A. Baseggio Conrado, S. Fanelli, V.A. McGuire, S.H. Ibbotson, Role of hypotaurine in protection against UVA-induced damage in keratinocytes, Photochem. Photobiol. 97 (2021) 353–359, https://doi.org/10.1111/php.13334.
[11] J. Chen, J. Luo, Y. Tan, M. Wang, Z. Liu, T. Yang, X. Lei, Effects of low-dose ALA-PDT on fibroblast photoaging induced by UVA irradiation and the underlying mechanisms, Photodiagnosis Photodyn. Ther. 27 (2019) 79–84, https://doi.org/10.1016/j.pdpdt.2019.05.006.
[12] Y. Ding, C. Jiratchayamaethasakul, S.H. Lee, Protocatechuic aldehyde attenuates UVA-induced photoaging in human dermal fibroblast cells by suppressing MAPKs/AP-1 and NF-kappaB signaling pathways, Int. J. Mol. Sci. 21 (2020), https://doi.org/10.3390/ijms21134619.
[13] S. Chen, Z. He, J. Xu, Application of adipose-derived stem cells in photoaging: basic science and literature review, Stem Cell Res. Ther. 11 (2020) 491, https://doi.org/10.1186/s13287-020-01994-z.
[14] M. Deng, Y. Xu, Z. Yu, X. Wang, Y. Cai, H. Zheng, W. Li, W. Zhang, Protective effect of fat extract on UVB-induced photoaging in vitro and in vivo, Oxid. Med. Cell. Longev. 2019 (2019) 6146942, https://doi.org/10.1155/2019/6146942.
[15] Y. Lin, Z. Cao, T. Lyu, T. Kong, Q. Zhang, K. Wu, Y. Wang, J. Zheng, Single-cell RNA-seq of UVB-radiated skin reveals landscape of photoaging-related inflammation and protection by vitamin D, Gene 831 (2022) 146563, https://doi.org/10.1016/j.gene.2022.146563.
[16] J. Liu, L. Liu, J. He, Y. Xu, Y. Wang, Multi-omic analysis of altered transcriptome and epigenetic signatures in the UV-induced DNA damage response, DNA Repair 106 (2021) 103172, https://doi.org/10.1016/j.dnarep.2021.103172.
[17] M. Robinson, P. Shah, Y.H. Cui, Y.Y. He, The role of dynamic m(6) A RNA methylation in photobiology, Photochem. Photobiol. 95 (2019) 95–104, https://doi.org/10.1111/php.12930.
[18] Y. Xiang, B. Laurent, C.H. Hsu, S. Nachtergaele, Z. Lu, W. Sheng, C. Xu, H. Chen, J. Ouyang, S. Wang, et al., RNA m(6)A methylation regulates the ultraviolet-induced DNA damage response, Nature 543 (2017) 573–576, https://doi.org/10.1038/nature21671.
[19] S. Zaccara, R.J. Ries, S.R. Jaffrey, Reading, writing and erasing mRNA methylation, Nat. Rev. Mol. Cell Biol. 20 (2019) 608–624, https://doi.org/10.1038/s41580-019-0168-5.

[20] S. Geula, S. Moshitch-Moshkovitz, D. Dominissini, A.A. Mansour, N. Kol, M. Salmon-Divon, V. Hershkovitz, E. Peer, N. Mor, Y.S. Manor, et al., Stem cells. m6A mRNA methylation facilitates resolution of naive pluripotency toward differentiation, Science 347 (2015) 1002–1006, https://doi.org/10.1126/science.1261417.
[21] X. Wang, Z. Lu, A. Gomez, G.C. Hon, Y. Yue, D. Han, Y. Fu, M. Parisien, Q. Dai, G. Jia, et al., N6-methyladenosine-dependent regulation of messenger RNA stability, Nature 505 (2014) 117–120, https://doi.org/10.1038/nature12730.
[22] S. Ke, E.A. Alemu, C. Mertens, E.C. Gantman, J.J. Fak, A. Mele, B. Haripal, I. Zucker-Scharff, M.J. Moore, C.Y. Park, et al., A majority of m6A residues are in the last exons, allowing the potential for 3' UTR regulation, Genes Dev. 29 (2015) 2037–2053, https://doi.org/10.1101/gad.269415.115.
[23] S. Ke, A. Pandya-Jones, Y. Saito, J.J. Fak, C.B. Vagbo, S. Geula, J.H. Hanna, D.L. Black, J.E. Darnell Jr., R.B. Darnell, m(6)A mRNA modifications are deposited in nascent pre-mRNA and are not required for splicing but do specify cytoplasmic turnover, Genes Dev. 31 (2017) 990–1006, https://doi.org/10.1101/gad.301036.117.
[24] H. Shi, J. Wei, C. He, Where, when, and how: context-dependent functions of RNA methylation writers, readers, and erasers, Mol Cell 74 (2019) 640–650, https://doi.org/10.1016/j.molcel.2019.04.025.
[25] W. Xu, C. He, E.G. Kaye, J. Li, M. Mu, G.M. Nelson, L. Dong, J. Wang, F. Wu, Y.G. Shi, et al., Dynamic control of chromatin-associated m(6)A methylation regulates nascent RNA synthesis, Mol Cell 82 (2022) 1156–1168 e1157, https://doi.org/10.1016/j.molcel.2022.02.006.
[26] J. Liu, Y. Yue, D. Han, X. Wang, Y. Fu, L. Zhang, G. Jia, M. Yu, Z. Lu, X. Deng, et al., A METTL3-METTL14 complex mediates mammalian nuclear RNA N6-adenosine methylation, Nat. Chem. Biol. 10 (2014) 93–95, https://doi.org/10.1038/nchembio.1432.
[27] Z. Yang, S. Yang, Y.H. Cui, J. Wei, P. Shah, G. Park, X. Cui, C. He, Y.Y. He, METTL14 facilitates global genome repair and suppresses skin tumorigenesis, Proc Natl Acad Sci U S A 118 (2021), https://doi.org/10.1073/pnas.2025948118.
[28] L. Marrot, Pollution and sun exposure: a deleterious synergy. Mechanisms and opportunities for skin protection, Curr. Med. Chem. 25 (2018) 5469–5486, https://doi.org/10.2174/0929867324666170918123907.
[29] K.J. Gromkowska-Kepka, A. Puscion-Jakubik, R. Markiewicz-Zukowska, K. Socha, The impact of ultraviolet radiation on skin photoaging - review of in vitro studies, J. Cosmet. Dermatol. 20 (2021) 3427–3431, https://doi.org/10.1111/jocd.14033.
[30] H. Jiang, X. Zhou, L. Chen, Asiaticoside delays senescence and attenuate generation of ROS in UV-exposure cells through regulates TGF-beta1/Smad pathway, Exp. Ther. Med. 24 (2022) 667, https://doi.org/10.3892/etm.2022.11603.
[31] J.M. Jung, O.Y. Kwon, J.K. Choi, S.H. Lee, Alpinia officinarum Rhizome ameliorates the UVB induced photoaging through attenuating the phosphorylation of AKT and ERK, BMC Complement Med Ther 22 (2022) 232, https://doi.org/10.1186/s12906-022-03707-w.
[32] S. Letsiou, Tracing skin aging process: a mini- review of in vitro approaches, Biogerontology 22 (2021) 261–272, https://doi.org/10.1007/s10522-021-09916-z.
[33] M. Gerasymchuk, V. Cherkasova, O. Kovalchuk, I. Kovalchuk, The role of microRNAs in organismal and skin aging, Int. J. Mol. Sci. 21 (2020), https://doi.org/10.3390/ijms21155281.
[34] K.W. Min, R.W. Zealy, S. Davila, M. Fomin, J.C. Cummings, D. Makowsky, C.H. McDowell, H. Thigpen, M. Hafner, S.H. Kwon, et al., Profiling of m6A RNA modifications identified an age-associated regulation of AGO2 mRNA stability, Aging Cell 17 (2018) e12753, https://doi.org/10.1111/acel.12753.
[35] M. Ouyang, J. Fang, M. Wang, X. Huang, J. Lan, Y. Qu, W. Lai, Q. Xu, Advanced glycation end products alter the m(6)A-modified RNA profiles in human dermal fibroblasts, Epigenomics 14 (2022) 431–449, https://doi.org/10.2217/epi-2022-0016.
[36] G. Ciossani, K. Overlack, A. Petrovic, P.J. Huis In 't Veld, C. Koerner, S. Wohlgemuth, S. Maffini, A. Musacchio, The kinetochore proteins CENP-E and CENP-F directly and specifically interact with distinct BUB mitotic checkpoint Ser/Thr kinases, J. Biol. Chem. 293 (2018) 10084–10101, https://doi.org/10.1074/jbc.RA118.003154.
[37] D. Subramonian, T.A. Chen, N. Paolini, X.D. Zhang, Poly-SUMO-2/3 chain modification of Nuf2 facilitates CENP-E kinetochore localization and chromosome congression during mitosis, Cell Cycle 20 (2021) 855–873, https://doi.org/10.1080/15384101.2021.1907509.
[38] Y. Bao, C. Qian, M.Y. Liu, F. Jiang, X. Jiang, H. Liu, Z. Zhang, F. Sun, N. Fu, Z. Hou, et al., PRKAA/AMPKalpha phosphorylation switches the role of RASAL2 from a suppressor to an activator of autophagy, Autophagy 17 (2021) 3607–3621, https://doi.org/10.1080/15548627.2021.1886767.
[39] R.E. Miller, N. Uwamahoro, J.H. Park, PPM1B depletion in U2OS cells supresses cell growth through RB1-E2F1 pathway and stimulates bleomycin-induced cell death, Biochem. Biophys. Res. Commun. 500 (2018) 391–397, https://doi.org/10.1016/j.bbrc.2018.04.084.
[40] Y. Liu, M. Li, X. Lv, K. Bao, X. Yu Tian, L. He, L. Shi, Y. Zhu, D. Ai, Yes-associated protein targets the transforming growth factor beta pathway to mediate high-fat/high-sucrose diet-induced arterial stiffness, Circ. Res. 130 (2022) 851–867, https://doi.org/10.1161/CIRCRESAHA.121.320464.
[41] R. Li, Y. Liang, B. Lin, Accumulation of systematic TPM1 mediates inflammation and neuronal remodeling by phosphorylating PKA and regulating the FABP5/NF-kappaB signaling pathway in the retina of aged mice, Aging Cell 21 (2022) e13566, https://doi.org/10.1111/acel.13566.
[42] W. Li, B. Cheng, Knockdown of LncRNA NEAT1 inhibits myofibroblast activity in oral submucous fibrosis through miR-760/TPM1 axis, J. Dent. Sci. 17 (2022) 707–717, https://doi.org/10.1016/j.jds.2021.11.003.